18^{th} Australasian Wind Engineering Society Workshop
McLaren Vale, Australia
06-08 July 2016

A study of transmission line cascades triggered by conductor breakage and wind loads

F. Alminhana[1,2], F. Albermani[1] and M. S. Mason[1]

[1]School of Civil Engineering, The University of Queensland, Queensland 4072, Australia
[2] Science and Technology Foundation - CIENTEC, Rio Grande do Sul, Brazil

Abstract

Cascades have played a major role in numerous serious transmission lines (TL) accidents around the globe. They are particularly prone to occurring in the presence of strong winds. During longitudinal cascades, the failure of a line component overloads the system, inducing a progressive failure that can involve many TL supports. Conductor breakage is regarded as a severe cascade triggering event, as it produces large shock waves that propagate throughout the line section and generate significant peak dynamic loads.

In this research, a mechanical model based on time-domain dynamic analysis was developed to predict the response of multi-span line sections under combined wind and conductor breakage loading. The model employs an explicit solution scheme that accounts for geometric and material nonlinearities. Correlated wind loads are simulated across the entire TL system with turbulent fluctuations based on an autoregressive moving average process.

This paper presents a case study where a transmission line with a history of structural failures is subjected to combined conductor breakage and wind action. The results indicated that the line suspension towers are able to contain longitudinal cascades in severe wind conditions.

Introduction

Cascades that occur during extreme wind and ice storms are commonly understood to be the major cause of severe transmission line accidents worldwide (CIGRÉ, 2012). These events result in lengthy and expensive power outages. Transmission line cascades are commonly classified into three categories, according to the direction of the damages, namely: longitudinal, transverse and vertical.

Longitudinal cascades are often the most severe type. They induce shock waves on transmission line conductors and shield wires, resulting in large unbalanced longitudinal loads on TL supports. They are usually triggered by a conductor breakage, although generally they can be initiated by the failure of any of the components required for maintaining tension in the line components.

The abrupt breakage of a conductor changes the boundary conditions of the line section in the severed span. Determination of the response in such conditions is relatively challenging, because the global stiffness matrix becomes singular, making conventional structural matrix analysis difficult to employ.

A mechanical model, described by Alminhana et al (2015b), was developed to numerically simulate the dynamic response of multi-span line sections subjected to conductor breakage loads, as a first stage of a broader investigation on TL cascades. The model couples the main line components and solves the equations of motion through an explicit integration scheme.

In the first version of the model, inelastic material behaviour of the tower members was not included and only geometric nonlinearities due to continuing changes in geometry were accounted for. This allows detection of overloaded members, and can be employed to design or retrofit line sections where it is desired that the supports withstand the peak dynamic loads (PDL) within the elastic range.

In order to more accurately determine the failure mode of TL supports and track structural damage propagation during a cascade event the existing mechanical model has recently been updated. A beam-column type element for transmission line lattice supports was introduced. This modification allows the inclusion of material and geometric due accumulated stresses nonlinearities.

Furthermore, wind loads for time-domain dynamic analysis are now automatically generated by simulating correlated time-dependent speeds at points attached to the joints of the line section. Time-dependent velocity profiles can be manipulated to represent extratropical cyclone or downburst wind events.

This paper investigates the behaviour of a 230 kV transmission line system when subjected to combined conductor breakage and/or wind load. This line is located in south Brazil and has suffered two major accidents since its construction in 1983. The response of a eight-span segment of the line was obtained for three load cases, including the combination of severe wind loading and conductor breakage.

Mechanical model

The mechanical model developed is designed to analyse complete transmission line sections. Each section is simulated as a group of three basic types of substructures: cable spans, supports and insulator sets. In turn, each substructure is formed by an assembly of basic members: cable (conductor and shield wire spans), tension-only (insulators), truss and beam-column (lattice supports) elements.

The formulation adopted for cable, truss and tension-only elements is described by Alminhana et al (2015a). The beam-column elements added to the model are straight rods with two joints and six degrees-of-freedom (DOFs) per joint, three translations and three rotations. Inelastic zones are defined at the element ends where plastic hinges can form. All material is assumed to be elastic-perfectly plastic. The element end forces are determined incrementally, through a tangent stiffness matrix in which the well-known linear-elastic stiffness matrix for frame elements $\mathbf{K}_L$ is augmented by a geometric and a plastic reduction matrices, $\mathbf{K}_G$ and $\mathbf{K}_P$, respectively, resulting in the following relation:

$$\mathbf{dF} = [\mathbf{K}_L + \mathbf{K}_G + \mathbf{K}_P]\,\mathbf{du} \tag{1}$$

where **dF** is the member end force increment and **du** the relative displacement between two consecutive time-steps.

The geometric stiffness matrix $\mathbf{K}_G$ accounts for the change in stiffness due to the effects of finite deformation and displacements, allowing the detection of members buckling. The matrix $\mathbf{K}_P$ restricts member end forces to plastic limits, which are

defined through a yield surface function Φ. The procedures to obtain the matrices $\mathbf{K}_L$, $\mathbf{K}_G$ and $\mathbf{K}_P$ are described by Albermani (1990). The function Φ can be used as a measure of member's safety in ultimate limit state: $0 \leqslant \Phi < 1$ means that the member internal forces are within the elastic range, whereas $\Phi = 1$ indicates the formation of plastic hinges.

The dynamic response of structural systems is obtained by solving the equations of motion. For linear elastic multi-degree-of-freedom systems with viscous damping these equations are well-known and can be written in a convenient matrix format:

$$\mathbf{M}\ddot{\mathbf{u}} + \mathbf{C}\dot{\mathbf{u}} + \mathbf{K}\mathbf{u} = \mathbf{P} \tag{2}$$

where: $\mathbf{M}$, $\mathbf{C}$ and $\mathbf{K}$ are the global matrices of mass, viscous damping and stiffness of the structure, respectively; $\ddot{\mathbf{u}}$, $\dot{\mathbf{u}}$ and $\mathbf{u}$ are the time-dependent vectors of acceleration, velocity and displacements; and $\mathbf{P}$ is the vector of applied forces, also time dependent.

The global stiffness is a function of time in the case of non-linear systems. The matrix $\mathbf{K}$ is also affected in the case of removal of failed members during the analysis, as a part of the system turns into a mechanism, causing $\mathbf{K}$ to become singular. Because $\mathbf{K}$ evolves during the analysis, the application of a frequency-domain approach is not suited, and a time-stepping scheme (direct integration) is required to achieve a solution.

An explicit integration method based on a central finite difference scheme was selected to determine structural response in the model described. A lumped-mass approach is adopted, resulting in a diagonalized matrix $\mathbf{M}$. A damping proportional to mass is assumed so the matrix $\mathbf{C}$ also becomes diagonal. These two artifices uncouple equation (2), since the stiffness matrix $\mathbf{K}$ multiplies a known vector of displacements from the previous iteration.

As a consequence, the system can be solved independently for each DOF, according to the following recurring formula:

$$u_{i+1} = \frac{1}{2+\alpha c_m \Delta t}\left[\frac{(1+\alpha)\alpha\,(p_i - \sum_{j=1}^{N} f_i^j)\Delta t^2}{m} + \right.$$
$$\left. + 2(1+\alpha)u_i - (2 - c_m\Delta t)\,\alpha\, u_{i-1}\right] \tag{3}$$

where u_{i+1}, u_i and u_{i-1} are displacements at time steps $(i+1)$, i and $(i-1)$, of a given DOF; m is the nodal mass; c_m is the proportionality constant between damping coefficient and nodal mass; p_i is the external load applied on the DOF and $\sum_{j=1}^{N} f_i^j$ is the sum of the end forces f_i of the N members connected to a node.

The parameter $\alpha = \Delta t_{i+1}/\Delta t_i$, that is, the ratio between two consecutive time steps, was introduced in Eq. (3) to permit changes in the time step during the analysis. As members enter the inelastic regime, it is necessary to assure that the transition between elastic and plastic zones is not abrupt and that the force increments in the inelastic regime do not drift significantly from the yield surface, which could result in a lack of accuracy in the solution. Strategies based on the reduction of Δt were devised to control these problems.

The central finite difference method is conditionally stable, producing meaningless results if the time step adopted is not short enough. Convergence criteria for the method are discussed by Alminhana et al (2015a). Despite this limitation, this approach is still efficient compared with equivalent implicit methods. The latter requires equilibrium check at each iteration due to the adoption of much larger time steps, and does not handles parallel computing easily, which plays a crucial role in dealing with the solution of structural systems with a large number of DOFs. In the model presented, parallel schemes were introduced at key points of the algorithm, dropping the total processing time of multiple-support line sections to a time comparable to that needed to achieve the solution of a single support.

Wind Load Generation

An event-based approach is used to automatically generate wind loads during the analysis. This allows the investigation of line section response under distinct storm scenarios. Loads are based on wind speed time-histories simulated at selected structural joints. The total velocity vector $\mathbf{U}$ at any point $\mathbf{P}$ of a wind field can be idealised as the sum of a slowly varying mean $\bar{\mathbf{U}}$ and turbulent $\mathbf{u}$ component, as:

$$\mathbf{U}(\mathbf{P},t) = \bar{\mathbf{U}}(\mathbf{P},t) + \mathbf{u}(\mathbf{P},t) \tag{4}$$

For extratropical cyclones, $\bar{\mathbf{U}}$ can be represented through the well-known logarithmic law. The turbulent component $\mathbf{u}$ is obtained through stochastic process theory. Different methods are available for simulating correlated turbulent speed components. The main purpose of these methods is to generate wind time histories, whose statistical properties match those of natural wind.

An AutoRegressive Moving Average (ARMA) method was selected. The stochastic processes simulated are assumed as stationary with a Gaussian distribution, compatible with the characteristics of extratropical cyclone winds. Each new value is added to the process by weighting a number of past values using cross-correlation matrices. The weighted values are summed together along with random shocks. The number of past values used in the calculation gives the order of the method. The approach is highly computationally efficient, as it requires only the storage of a set of coefficients and a white noise source after an initial phase of calculations. A description of the method derivation is provided by Samaras et al (1985).

The algorithm developed generates longitudinal, lateral and vertical turbulent fluctuations through multiple stochastic processes. Coefficients of the ARMA cross-correlation matrices are calculated based on the power spectral density functions of Kaimal et al (1972). Spatial correlation decay is accounted for with the empirical model of Davenport (1968). Figure 1 depicts a plot of a simulated 30 s record of a along-wind speed component.

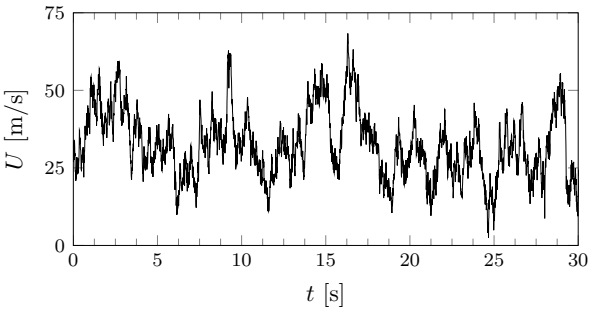

Figure 1: Simulated 30 s record of along-wind speed.

The procedures indicated in the standard IEC60826, IEC (2003), were adapted to calculate the effective wind load on the line components, according to wind speed time-histories. The original formulation was transformed into a vectorial form in order to couple the calculated loads into the dynamic analysis.

Case study

An eight-span section of a 230 kV single circuit transmission line in south Brazil was selected for this case study. This line connects electrical substations in the cities of Pelotas and Rio Grande, which are located next to the Atlantic ocean with a latitude around 30S. The total length of the line is 45 km, crossing mostly flat open terrain.

The line has a total of 103 supports with an average span around 466 m. It was constructed in 1983 and has suffered two major accidents during wind storms up to the present. In the first, the felling of three line supports was reported by Silva (1991). The second event, illustrated in Figure 2, involved the collapse of five supports during downburst winds in 2006 (Silva, 2006).

Figure 2: Failed tower on the investigated line following a downburst event in 2006.

Three conductor phases and two shield wires compose the transmission system. Each conductor phase is formed by a single Aluminium Cable Steel Reinforced (ACSR) type conductor, with the commercial name Grosbeak. All phases are sagged according to an everyday stress condition (EDS): average temperature of 20 °C and no wind; catenary parameter of $C = 1755$ m, equivalent to a horizontal tension of $H = 22.43$ kN.

The shield wires are $3/8''$ high strength steel (HS) cables, sagged in an EDS condition with $C = 1950$ m, resulting in an axial tension with horizontal component of $H = 7.80$ kN. The suspension insulators are single I-string type with a length of 2.6 m for all conductor phases.

Supports are freestanding delta-type steel lattice towers. Suspension towers, named FS, varies from 19.4 m to 34.4 m in total height. They are square based with side lengths ranging from 4.2 m to 7.5 m. The self-weight of the shortest tower is 25.7 kN, while the tallest is 48.5 kN. All members are structural steel angle sections of grades 345 MPa or 413 MPa.

Nearly half of the line supports are within a very long tension section that encompasses 45 supports. The line segment between supports 44 and 52, which was affected during the last accident, was used to investigate the TL response to conductor breakage during extratropical cyclonic winds. The end towers of the segment were replaced by rigid supports. Although the height of the supports varies about 1 m in this segment, a tower with uniform height (FS24) was adopted. Figure 3 illustrates the simulated segment.

The natural frequencies of the FS24 tower were determined using an auxiliary routine based on the Lanczos-Ritz method. The first three natural frequencies are 3.64 Hz, 3.78 Hz and 6.98 Hz, corresponding to the lateral, longitudinal and torsional modes, respectively. The natural frequencies of low-sagged cables can be determined analytically. Assuming a levelled span of 450 m, the lowest frequency for the in-plane mode shapes is around 0.30 Hz for both conductors and shield wires.

No damping test data is available for this tower. Experimental measurements conducted by Silva et al (1984) suggest damping ratio ranging from $\zeta = 3\%$ to $\zeta = 6\%$ for similar lattice towers vibrating within the elastic regime. Experimental data for conductor and shield wire damping is also limited.

An overall mass-proportional constant of $c_m = 2.5\,\mathrm{s}^{-1}$ was adopted for the towers and $c_m = 0.02\,\mathrm{s}^{-1}$ for cables, equivalent to a damping ratio of $\zeta = 5\%$ (towers) and $\zeta = 0.5\%$ (cables), approximately. Aerodynamic damping is automatically accounted for in the model based on the speed of the structural joints.

Wind speed recordings were obtained from a meteorological station located in the city of Pelotas. The yearly maximum speeds averaged over 10 min at a reference height of 10 m were available for a period of 33 years. Analysing these data, a mean speed of $15.59\,\mathrm{ms}^{-1}$ and coefficient of variation of 21.69% were determined. These records were fitted with a Gumbel extreme probability distribution to obtain the reference wind speed employed in this investigation.

A roughness length of $z_o = 0.04$ corresponding to a grassland terrain was adopted when simulating the oncoming wind field. An interval of $\Delta\tau = 5 \times 10^{-2}$s was used to generate wind-speed time histories with an ARMA of order 3. A time-step interval $\Delta t = 2 \times 10^{-4}$s was assumed at the start of the dynamic analysis and automatically adjusted to reduced values as the end forces in the most loaded members approach the yield surface.

Response of the line section was determined for the following loading conditions:

- LC1 An extratropical cyclone wind field acting transversally to the line is simulated - reference speed $V_r = 28\,\mathrm{ms}^{-1}$ ($T = 100$ years return period). Conductors are maintained intact.

- LC2 Conductor breakage is simulated under EDS condition. No wind load is applied.

- LC3 A wind load is applied to the line section, as described for LC1. The return period of the wind is $T = 250$ years - $V_r = 31\,\mathrm{ms}^{-1}$. The conductor breakage is simulated.

The lateral phase (left) was selected to be severed, in order to include torsional effects. Breakage was simulated by removing the cable element attached to the insulator of support 46 (2^{nd} span), as indicated in Figure 3.

Results

For LC1, the response of the intact line was assessed to updated design conditions, in accordance with the limit states criteria. The design of the tower FS is dated from 1971 and was based on simplified wind load procedures, still adopting the working stress approach. The nonlinear dynamic analysis showed that the line behaved safely for ultimate limit state loads, since all supports remained within the elastic range. The largest values of the yield surface function ($\Phi_{max} \cong 0.8$) occurred in members of support 45, which has the longest wind span in the line section.

For LC2, the effects of conductor breakage loads remained confined to the support (46), closest to the severed cable member. This support was able to absorb the peak dynamic load (PDL) imposed by the intact span, around 68 kN, with damages limited to a few members located at the tower's beam. The tower FS was originally designed for a residual static load (RSL) of 30 kN combined with wind of $T = 100$year return period, which explain its safe behaviour in this simulation. A total number of 20 members were affected only.

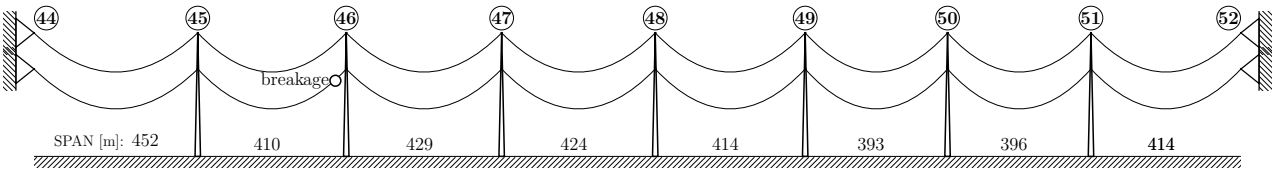

Figure 3: Profile of the simulated transmission line section.

In the LC3, the impact loads were also contained by support 46, at the expense of the failure of a large number of the members of the tower's beam and cross-arms. Members in the tower top and main body were also compromised (Figure 4). Supports 45 and 47 suffered slight damage in beam members, and none of the other towers were affected. The peak dynamic load reached 82 kN in the conductors. A total number of 81 members failed in support 46.

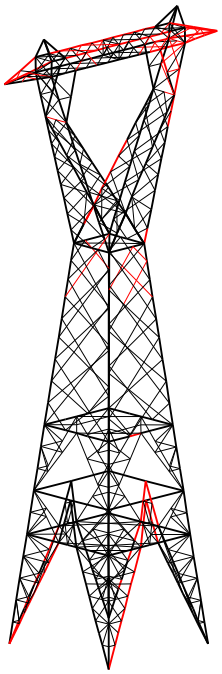

Figure 4: Support 46 deformed shape and failed members (red).

Conclusions

This article described a numerical model to analyse multi-span transmission line sections. A time-dependent nonlinear dynamic analysis was adopted. The main line components are fully simulated. Beam-column elements capable of detecting buckling and hinge plastic formation were introduced to track post-elastic behaviour of TL supports. Wind loads for the dynamic analysis are automatically generated, based on correlated speeds within a wind field.

The behaviour of a transmission line design based on working stress criteria which has been involved in two major accidents was investigated using the developed model. The response of the intact line under ultimate limit state loads indicates that the supports perform safely according to the limit state method.

The nonlinear dynamic analysis revealed that the suspension structures employed in the line are able to contain longitudinal failure propagation of one conductor phase in severe wind conditions, by using tower's post-elastic reserve. This is compatible with current transmission line design practice adopted by many utilities, where the failure of a few suspension supports is accepted as long as cascades are contained.

Acknowledgements

The authors wish to thank Engineer Vilson Renato da Silva for kindly lending the report of the second accident and other related documents of the TL investigated in this paper, and CNPq - Brazilian National Council for Scientific and Technological Development - for financial support. *

References

Albermani FGA (1990) Towards nonlinear analysis of transmission tower structures. Thesis, The University of Queensland

Alminhana F, Albermani F, Mason M (2015a) Comparison of Responses of Guyed and Freestanding Transmission Line Towers Under Conductor Breakage Loading. Int J Struct Stab Dyn p 1540023, DOI 10.1142/S0219455415400234

Alminhana F, Albermani F, Mason M (2015b) Dynamic Analysis of a Transmission Line Section Subject to Combined Conductor Breakage and Wind Loads. In: 17th Australas. Wind Eng. Soc. Work., pp 1–4

Chay MT, Albermani F, Wilson R (2006) Numerical and analytical simulation of downburst wind loads. Eng Struct 28(2):240–254

CIGRÉ (2012) Brochure 515 - Mechanical Security of Overhead Lines: Containing Cascading Failures and Mitigating Their Effects. Tech. rep.

Davenport AG (1968) The Dependence of Wind Loads on Meteorological Parameter. Wind Eff Build Struct pp 19–82

IEC (2003) IEC 60826 - Design Criteria of Overhead Transmission Lines. International Electro Technical Commission

Kaimal JCJ, Wyngaard JCJ, Izumi Y, Coté OR, Cote OR (1972) Spectral Characteristics of Surface-Layer Turbulence. Q J … 98(417):563–589

Samaras E, Shinzuka M, Tsurui A (1985) ARMA Representation of Random Processes. J Eng Mech 111(3):449–461, DOI 10.1061/(ASCE)0733-9399(1985)111:3(449)

Silva VR (2006) Relatório da Visita de Inspeção do Acidente com a LT 230 KV QUINTA- PELOTAS 3. Tech. rep., Porto Alegre

Silva VR, Elias RdA (1991) Desempenho Estrutural de LTs do Sistema CEEE Segundo Differentes Procedimentos de Cálculo de Cargas de Vento. In: XI Semin. Nac. Produção e Transm. Energ. Elétrica, Rio de Janeiro

Silva VR, Riera JD, Joaquim Blessman, Nani LF, Galindez EE (1984) Determinação Experimental das Propriedades Dinâmicas Básicas de uma Torre de Transmissão de 230 kV. In: VII Semin. Nac. Produção e Transm. Energ. Elétrica, Brasilia, p 10